Paleoceanography and Paleoclimatology

RESEARCH ARTICLE
10.1029/2025PA005108

Expanded Composite Coral Indices of South Pacific Convergence Zone Oceanographic Variability Since 1848 CE

Sara Todorović[1,2], Braddock K. Linsley[3], Henning Kuhnert[4], Delphine Dissard[5], Christophe Menkes[6], and Henry C. Wu[1]

[1]Leibniz Centre for Tropical Marine Research (ZMT), Bremen, Germany, [2]Faculty of Geosciences, University of Bremen, Bremen, Germany, [3]Lamont-Doherty Earth Observatory of Columbia University, Palisades, NY, USA, [4]MARUM – Center for Marine Environmental Sciences, University of Bremen, Bremen, Germany, [5]IRD UMR LOCEAN (IRDCNRS-MNHN-Sorbonne Universités, CNRS-MNHN), Nouméa/Paris, France, [6]ENTROPIE (IRD, University of New Caledonia, University of La Réunion, CNRS, Ifremer), Nouméa, New Caledonia

Abstract In the South Pacific Convergence Zone (SPCZ), interannual to interdecadal oceanic and atmospheric variability is especially pronounced. The El Niño Southern Oscillation and the Interdecadal Pacific Oscillation significantly influence the SPCZ diagonal axis and salinity front. Regional coral-based paleo-environmental reconstructions extend the relatively short and discontinuous instrumental sea surface temperature (SST) and sea surface salinity (SSS) record to elucidate past variability. We present monthly resolved, composite indices of coral skeletal $\delta^{18}O$, Sr/Ca, and calculated $\delta^{18}O_{sw}$ utilizing coral geochemical time-series from Rotuma, Fiji, Tonga, and Rarotonga, dubbed the $SPCZ_{coral}$ ($SPCZ_c$) indices. The new indices build upon previous efforts to describe variability and trends in the SPCZ region with expanded coverage due to a new northwestern coral addition from the SPCZ fresh pool. The increased spatial and temporal resolution of the new indices allows for higher-fidelity sub-annual reconstructions of SST and SSS in the region dating back to 1848. The results confirm the secular warming trend of 1°C in the SPCZ region and show a 0.4 S_p freshening starting in the 1880s. The $SPCZ_c$ $\delta^{18}O_{sw}$ is the first regional reconstruction of $\delta^{18}O_{sw}$ and provides valuable insights into past SSS variability, including elucidating responses to El Niño and La Niña events, as well as identifying past SPCZ zonal events. The $SPCZ_c$ $\delta^{18}O_{sw}$ reconstruction extends the instrumental records by ~100 years. The $SPCZ_c$ indices prove the utility of the compositing approach in describing regional oceanographic variability with the increased signal-to-noise ratio of the obtained coral climatic data.

Plain Language Summary The South Pacific Convergence Zone (SPCZ) is a significant rainfall and cloud band in the Southwest Pacific, acting as the most persistent extension of the Intertropical Convergence Zone (ITCZ). Its variability on interannual and decadal scales leads to droughts and floods in island nations due to fluctuating rainfall. Future climate projections, often inaccurately represented in models, are closely linked to this region's oceanic and atmospheric processes. Coral-based reconstructions ($SPCZ_{coral}$) extend limited instrumental sea surface temperature and ocean salinity data to the 1850s, documenting SPCZ variability and long-term trends. We find a 1°C warming and 0.4 S_p (salinity units) freshening over the last century. $SPCZ_c$ indices show pronounced responses to Eastern Pacific El Niño events, aiding in past event identification. Additionally, the $SPCZ_c$ salinity index allows reconstruction of past SPCZ zonal events, when its rainfall axis shifts toward the equator, causing droughts in southwestern islands. These insights improve understanding of SPCZ variability, enhancing future predictions.

Key Points:

- The new composite indices have an improved spatial coverage of the South Pacific Convergence Zone and increased temporal resolution
- We observe a warming of 1°C and freshening of 0.4 S_p in the South Pacific Convergence Zone in the past 150 years
- The indices provide accurate reconstruction of past interannual and decadal climate variability modes

Supporting Information:

Supporting Information may be found in the online version of this article.

Correspondence to:

S. Todorović,
sara.todorovic@leibniz-zmt.de

Citation:

Todorović, S., Linsley, B. K., Kuhnert, H., Dissard, D., Menkes, C., & Wu, H. C. (2025). Expanded composite coral indices of South Pacific Convergence Zone oceanographic variability since 1848 CE. *Paleoceanography and Paleoclimatology*, *40*, e2025PA005108. https://doi.org/10.1029/2025PA005108

Received 20 JAN 2025
Accepted 6 MAR 2025

Author Contributions:

Conceptualization: Sara Todorović, Henry C. Wu
Data curation: Henning Kuhnert
Formal analysis: Sara Todorović
Funding acquisition: Henry C. Wu
Methodology: Sara Todorović, Braddock K. Linsley
Project administration: Henry C. Wu
Resources: Braddock K. Linsley, Delphine Dissard
Supervision: Henry C. Wu
Visualization: Sara Todorović, Christophe Menkes
Writing – original draft: Sara Todorović
Writing – review & editing: Sara Todorović, Braddock K. Linsley,

1. Introduction

The tropical Southwest (SW) Pacific is home to the Southern Hemisphere sector of the Western Pacific Warm Pool (WPWP). The WPWP, dubbed the Earth's heat engine due to its large spatial extent and volume of 28–29°C seawater, is stratified down to a depth of 100 m (Wyrtki, 1989). The WPWP supplies the majority of the water vapor and latent heat to the atmosphere, leading to high cloudiness and strong convective precipitation in excess of 2–3 m of rain annually freshening the waters to <35 S_p (practical salinity units) (Chen et al., 2004; Delcroix et al., 1996). This area of high atmospheric convergence and convection is also the location of the South Pacific Convergence Zone (SPCZ). The SPCZ comprises a two-component system: a zonally oriented tropical high rainfall band over the WPWP, and diagonally oriented (northwest to southeast) rainfall band extending from the WPWP toward French Polynesia to approximately 30°S, 120°W (Brown et al., 2020; Vincent, 1994) (Figure 1b).

Henning Kuhnert, Delphine Dissard, Christophe Menkes, Henry C. Wu

The SPCZ salinity front separates the warm, fresh waters of the WPWP from the adjacent saltier and cooler waters. Interannual and interdecadal variability are the strongest modes of variability in the SPCZ after the seasonal cycle and can affect the orientation of the SPCZ diagonal axis (Brown et al., 2020; Power et al., 1999; Trenberth, 1976). The shifts in the SPCZ axis bring floods and droughts to different parts of the island nations of the region and affect tropical cyclogenesis (Higgins et al., 2023; Menkes et al., 2012; Vincent et al., 2011).

The strength and position of the SPCZ are strongly modulated by El Niño-Southern Oscillation (ENSO) on interannual timescales (Vincent et al., 2011). During an El Niño, the SPCZ maximum rainfall axis shifts northeast, which causes less rainfall and cooler sea surface temperatures (SST) in the region south of the mean SPCZ position (Brown et al., 2020). During some stronger El Niño years, the SPCZ maximum precipitation axis can shift to a zonal orientation, known as an SPCZ zonal event (Cai et al., 2012; Vincent et al., 2011). During La Niña events, the axis shifts slightly more southwestward compared to the neutral state. Over interdecadal timescales, the Interdecadal Pacific Oscillation (IPO) spatial and temporal patterns of Pacific-wide SST change also modulate SPCZ position as well as ENSO intensity (Folland et al., 2002). With its positive and negative phases, the IPO roughly parallels the phenomena of El Niño and La Niña, respectively (Henley et al., 2015). IPO is comparable, although not identical, to the North Pacific interdecadal variability, the Pacific Decadal Oscillation (PDO) (Newman et al., 2016). They both exhibit similar SST signatures (Folland et al., 2002; Power et al., 1999), but the North Pacific center of action is enhanced in IPO compared to PDO (Newman et al., 2016). Sometimes they are together referred to as the Pacific decadal variability (PDV) (Henley, 2017; Porter et al., 2021). Changes in SPCZ SST anomalies and position are felt way beyond the SW Pacific through teleconnections such as the Pacific North American teleconnection (PNA) that influences weather events in North America or via teleconnections to high southern latitudes to West Antarctic, and high northern latitudes to the Arctic where it modulates sea ice loss (Baxter et al., 2019; Bonan & Blanchard-Wrigglesworth, 2020; Clem et al., 2019). Despite its important role in modulating regional climate variability (Vincent et al., 2011), global circulation (Vincent, 1994), and ocean freshwater budget (Lorrey et al., 2012; Matthews, 2012), the in-situ observations of the SPCZ are spatially and temporally scattered, and reanalysis products are based on fewer observations prior to the 1980s (Davis et al., 2019; Huang et al., 2019, and references therein).

Climate reconstructions on a seasonal to monthly scale from massive corals can provide unique evidence of oceanographic variability over the past several centuries. The stable oxygen isotope composition ($\delta^{18}O$) of corals has been shown in many settings to be a reliable proxy reflecting both changes in SST and the $\delta^{18}O$ of seawater ($\delta^{18}O_{sw}$) (Thompson et al., 2022; Weber & Woodhead, 1972). In regions of high atmospheric convergence and rainfall, $\delta^{18}O_{sw}$ is highly correlated with sea surface salinity (SSS) and can be the primary driver of coral $\delta^{18}O$ variability (Fairbanks et al., 1997; LeGrande & Schmidt, 2006; Thompson et al., 2022). The Strontium-to-Calcium (Sr/Ca) ratio is a commonly used proxy for temperature (Corrège, 2006, and references therein). However, physiological and physicochemical processes can affect the temperature-driven partitioning of Sr in coral skeletons (Gaetani & Cohen, 2006; Sinclair et al., 2006). Recent studies have proposed an array of alternative methods to remove the non-temperature-related influences (DeCarlo et al., 2016; D'Olivo et al., 2018; Montagna et al., 2014; Wu et al., 2021). With these caveats in mind, Sr/Ca is well correlated with SST at many study sites across the Pacific over the late twentieth century instrumental period, and is the most extensively used SST proxy on *Porites* sp. corals. When paired, coral $\delta^{18}O$ and Sr/Ca ratios make it possible to separate the $\delta^{18}O_{sw}$ contribution to skeletal $\delta^{18}O$ and obtain a coral-based SSS proxy (Cahyarini et al., 2008; Ren et al., 2002). Existing coral-based climate reconstructions have provided invaluable insights into the variability of the SPCZ (Bagnato et al., 2005; Dassié et al., 2018; Linsley et al., 2008, 2015; Tangri et al., 2018; Wu et al., 2013). However, multi-centennial records of paired $\delta^{18}O$ and Sr/Ca are still rare.

To study regional variability, it is imperative to have replicated records from a representative area to obtain a reliable reconstruction (DeLong et al., 2007; Linsley et al., 2008). Regional decadal SST variability in relation to IPO and upper ocean heat content has been previously described from annual coral Sr/Ca values (Linsley et al., 2015). The study found the coral composite of Fiji-Tonga-Rarotonga (dubbed the FTR index) to capture accurately the past shifts in IPO phases and recent ocean heat content increase. Our study builds on this concept to investigate the coral response to interannual SST forcing and SSS variability in the SPCZ region. To achieve a representative sampling rate for elucidating interannual signals in coral reconstruction records, we included only

10.1029/2025PA005108

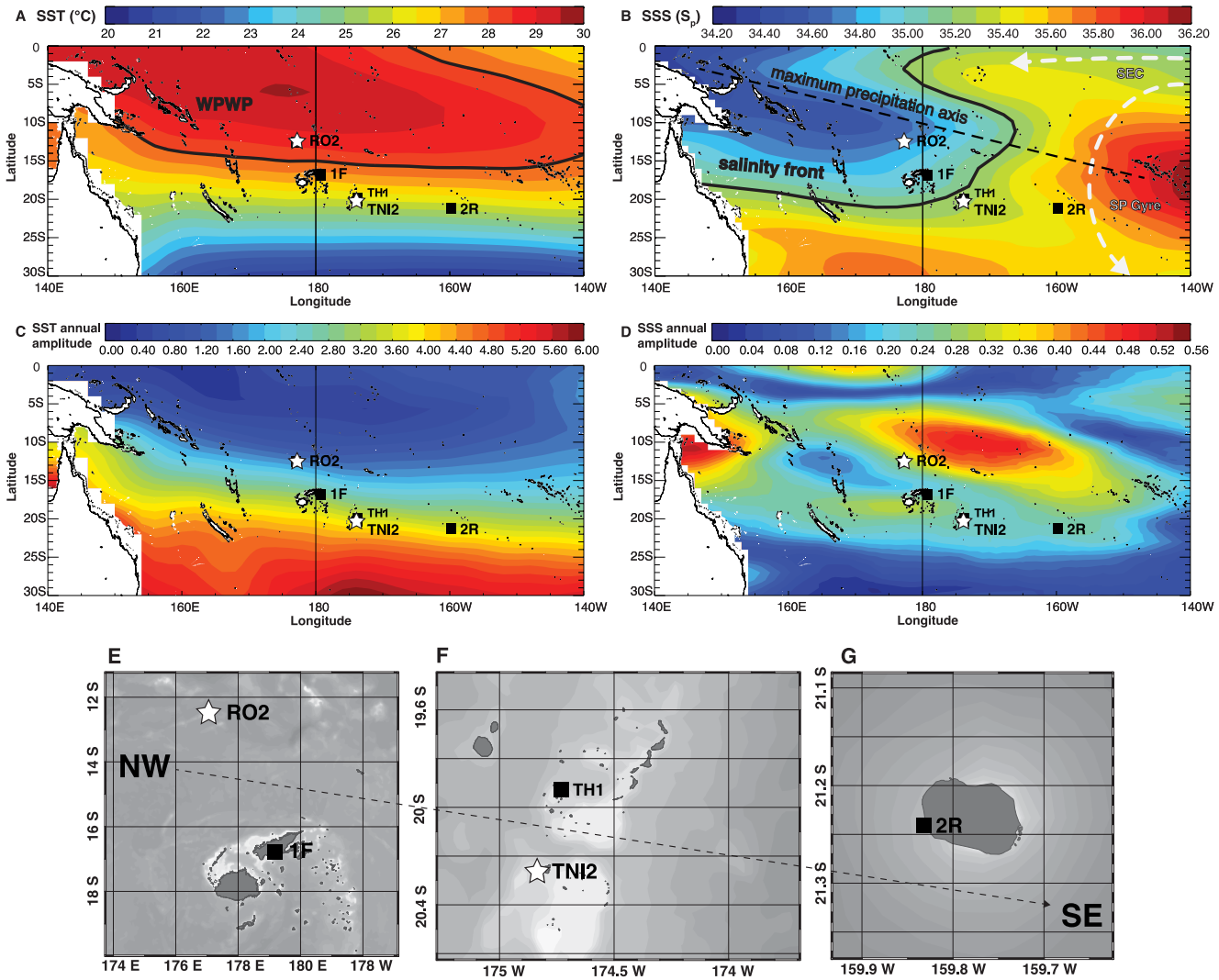

Figure 1. Study region map depicting the oceanographic conditions of the South Pacific. Map of the Southwest Pacific shaded with: (a) annual average SST (2° × 2° ERSST v4, Huang et al., 2015) where the Warm Pool is delineated by a 28°C isotherm in black; (b) annual average SSS (1° × 1° SSS dataset from Delcroix et al., 2011), with mean maximum precipitation of the SPCZ (Brown et al., 2020) shown with a dashed black line, and the 35.2 S_p isohaline (black line) delineating the mean extent of the SPCZ fresh pool. White dashed lines show the circulation patterns of the South Equatorial Current (SEC) and the South Pacific Gyre (SP Gyre) (adapted from Todorović, Wu, et al., 2024); (c) annual SST amplitude (ERSST v4, Huang et al., 2015); (d) annual SSS amplitude (1° × 1° SSS dataset from Delcroix et al., 2011). The shading in panels E, F, and G represents local bathymetry. (e) Corals from Rotuma and Fiji are in the fresh pool, with Rotuma additionally being located within the WPWP. (f) Tonga corals are 50 km apart. (g) Rarotonga coral is the southeastern member of the SPCZ coral network. Corals added to the existing SPCZ coral network are marked with stars.

the available sub-annually sampled coral records (Quinn et al., 1996; Vautard & Ghil, 1989). With coarser sampling resolution, the annual cycle amplitude decreases (DeLong et al., 2007). Summer minima and winter maxima are not fully captured in this case, and there is an overall information loss for studying interannual variability.

This study offers a reconstruction of climatic variability with spatially expanded regional coverage at high temporal resolution. We test the descriptive power of the newly introduced $SPCZ_{coral}$ ($SPCZ_c$) indices against instrumental gridded SST and SSS data from the region and illustrate their utility in reconstructing past variability at interannual and interdecadal scales. Our findings underscore the advantages of the compositing approach in reconstructing past oceanographic variability and the need for further coral-based regional replication studies.

2. Methods

2.1. Study Site

The corals included in the study are spatially distributed along the SPCZ diagonal axis (Figure 1) and cover approximately the area from 12° to 21°S and 177°E to 159°W to capture a broader extent of the regional variability. A comparison of the average climatology of all coral locations in this study using the 2° × 2° resolved Extended Reconstructed SST, version 4 (ERSST) (Huang et al., 2015), and Delcroix et al. (2011) SSS, captures a gradient of temperature and salinity across the northwest to the southeast (see Figure S1 in Supporting Information S1 for time series of seasonal variability). Rotuma exhibits the highest average annual temperature of 28.7°C but has the smallest average seasonal SST amplitude of only 1.7°C (Figure 1c). When moving diagonally southeast to Rarotonga from Rotuma, the annual average SST decreases to 25.5°C, and the average seasonal amplitude increases to 3.7°C. The salinity gradient increases from the northwest to the southeast. Rotuma and Fiji are distinctly in the SPCZ fresh pool (Figures 1b and 1e) within the 35.2 S_p isohaline, while Tonga and Rarotonga on the other side of the gradient (Figures 1b–1f and 1g). Seasonal cycles are strongest at Rotuma (0.6 S_p) and weaken toward Rarotonga (0.3 S_p) (Figure 1d). SSS variability increases over interannual timescales and ranges from approximately 1.2 S_p at Rarotonga to 2.0 S_p at Rotuma. Rotuma also has an overall higher annual average precipitation rate compared to the other three locations. Fiji, in contrast to the other locations, exhibits a stronger amplitude of seasonal variability between the rainy and dry seasons.

2.2. Instrumental Data

We use the Extended Reconstructed Sea Surface Temperature (ERSST) version 4 monthly product (Huang et al., 2015) for coral Sr/Ca to SST calibration for the period of 1950–1996, and additionally back to 1854, as the ERSST goes further back in time compared to other gridded SST datasets available (e.g., HadISST, OISST). For reconstructed $\delta^{18}O_{sw}$ to SSS calibration, the Delcroix et al. (2011) SSS (hereafter D-SSS) was used as it provides optimal coverage of the region, and additionally for comparison to other available datasets (Dassié et al., 2018; Todorović, Wu, et al., 2024). Instrumental data were extracted from the closest grid cell to each coral location (see Table S1 in Supporting Information S1). Composite instrumental indices for the SPCZ region were produced by averaging monthly SST and SSS data from these cells over the total number of cells, resulting in the time series shown in Figures 2a and 2b.

2.3. Coral Data

For this study, four *Porites* sp. coral cores (RO2, 1F, TNI2, 2R), sampled at four locations along the SPCZ diagonal axis (Figure 1, Table 1), are used to establish paleo-SST and SSS indices of monthly to interdecadal variability of the SPCZ region. Some of these coral cores (1F, TH1, 2R) have been previously used to establish the Sr/Ca-based annual Fiji-Tonga-Rarotonga (FTR) Index to constrain the South Pacific decadal SST variability from 1791 to 1997 (Linsley et al., 2015). Dassié et al. (2018) later used the same cores to constrain the SPCZ salinity front variability at each location from annual coral $\delta^{18}O$ values back to the 1880s.

To our knowledge, there are very few long modern coral-based reconstructions emanating from the WPWP south of the equator. Rotuma (RO2, Figure 1e) coral down-core Sr/Ca and $\delta^{18}O$ data are added to the ensemble as the new end-member from the fresh and warm pool to the previously published network of SPCZ corals (Figures 1e–1g) (Todorović, Dissard, et al., 2024; Todorović, Wu, et al., 2024). Thus, the addition of this coral to the SPCZ coral network offers a relatively singular and invaluable source of paleoenvironmental information for characterizing this region. We utilize Fiji (1F) and Rarotonga (2R) corals previously used in Linsley et al. (2015) annual composite reconstruction. We replace Tonga core TH1, used by Linsley et al. (2015), with Tonga coral core TNI2 because it offers a greatly extended monthly record (Todorović, Dissard, et al., 2024; Todorović, Wu, et al., 2024), as TH1's subannual sampling ends in 1944. Based on monthly interpolated Sr/Ca and $\delta^{18}O$ records of these four corals (RO2, 1F, TNI2, 2R), we present a highly resolved Sr/Ca-based composite reconstruction of SST, and a $\delta^{18}O_{sw}$ reconstruction of SSS from paired $\delta^{18}O$ and Sr/Ca measurements within the newly generated, spatially expanded $SPCZ_c$ indices.

Precise and detailed information regarding sampling, stable isotope analysis, trace element analysis, and chronology development for the coral cores included in this study can be found in their respective publications (Table 1).

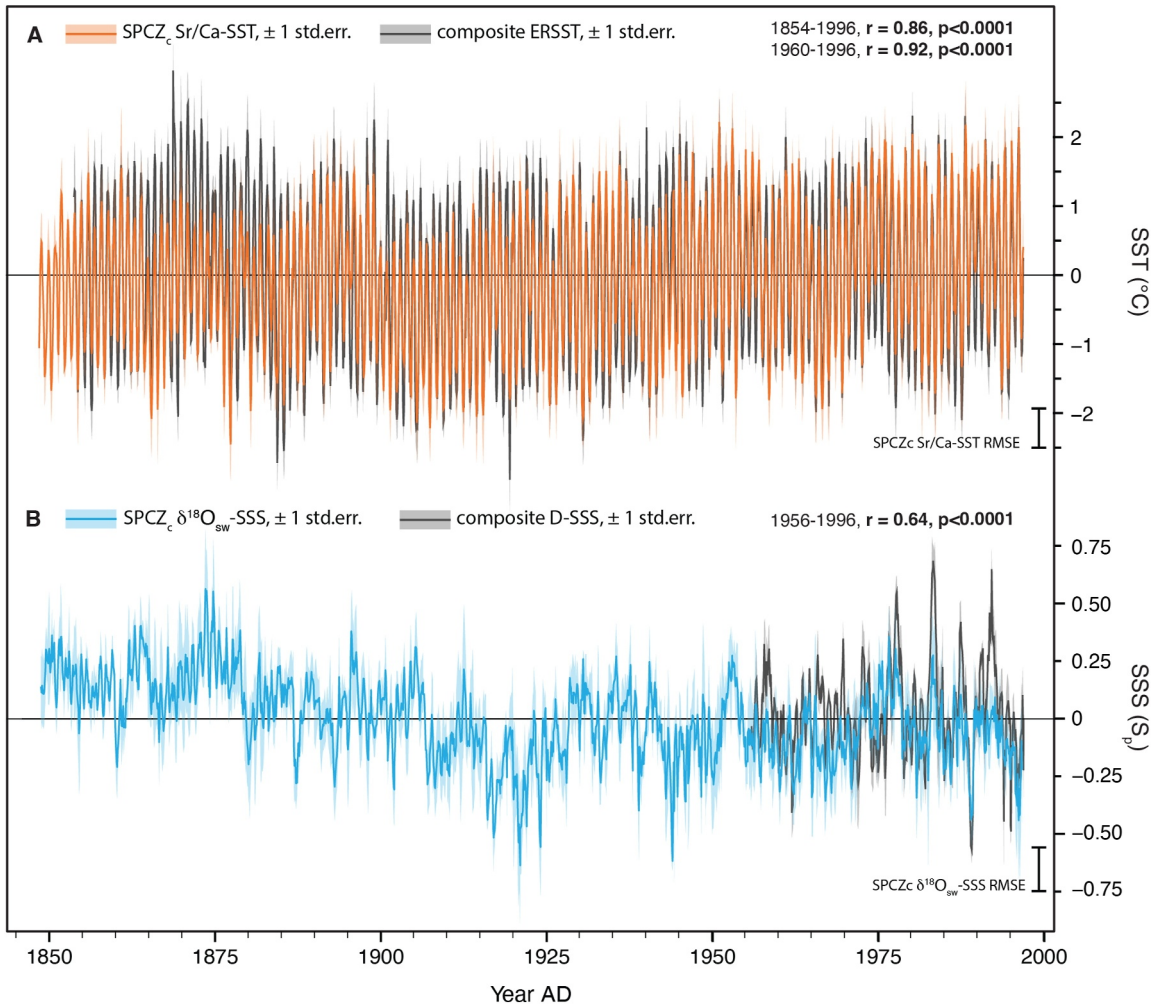

Figure 2. $SPCZ_c$ indices of SST and SSS: (a) $SPCZ_c$–SST is shown on top of the ERSST composite of the region. (b) $SPCZ_c$–SSS is shown on top of the D-SSS composite of the region. All composite indices are enveloped by ±1 s.e.

2.4. Construction of Composite Indices

All coral Sr/Ca and $\delta^{18}O$ records were interpolated to monthly resolution from mm-scale analyses. Previous studies have found that every other millimeter sampling does not attenuate or smooth the seasonal cycles in this region when a higher seasonal SST amplitude is present (Wu et al., 2013), providing confidence in extrapolating the less resolved eight samples/year (Fiji 1F coral) and nine samples/year (Rarotonga 2R coral) records to 12 samples/year. For the $\delta^{18}O_{sw}$ reconstruction, we used the Sr/Ca-SST slope obtained from the coral Sr/Ca-ERSST

Table 1
Coral Cores Included in the Study – Their Years of Record, Location of Coring and Publications Where They Were First Published

Core	Years	Location	Lat, lon	Published
RO2	1821–1998	Rotuma, Fiji	12°29'S, 177°06'E	Todorović, Dissard, et al., 2024, Todorović, Wu, et al., 2024
1F	1781–1997	Savusavu Bay, Fiji	16°49'S, 179°14'W	Linsley et al., 2004
TH1	1944–2004	Ha'afera Island, Tonga	19°56'S, 174°43'W	Linsley et al., 2008 Wu et al., 2013
TNI2	1848–2004	Nomuka Iki Island, Tonga	20°16'S, 174°49'W	Linsley et al., 2008 Todorović, Dissard, et al., 2024, Todorović, Wu, et al., 2024
2R	1726–1996	Rarotonga, Cook Islands	21°14'S, 159°49'W	Linsley et al., 2000, 2004

Table 2
Parameters Used in $\delta^{18}O_{sw}$ Reconstruction Following the Method of Ren et al., 2002

	RO2	1F	TNI2	2R
$\delta^{18}O$ to SST (‰ per ºC) ± s.e.	−0.19 ± 0.01	−0.15 ± 0.005	−0.15 ± 0.004	−0.13 ± 0.004
Sr/Ca to SST (mmol/mol per ºC) ± s.e.	−0.09 ± 0.004	−0.66 ± 0.001	−0.083 ± 0.002	−0.72 ± 0.002
Average $\delta^{18}O_{sw}$ (‰), LeGrande and Schmidt (2006)	0.349	0.433	0.498	0.610

Note. Sr/Ca records of each coral were regressed against ERSST for that location using the RMA regression method (1950 – end of each coral record). Similarly, $\delta^{18}O$ records were regressed against ERSST for each coral in the same period using the OLS regression.

Reduced Major Axis (RMA) regression, and the latest available gridded $\delta^{18}O_{sw}$ values (LeGrande & Schmidt, 2006), following the approach of Todorović, Wu, et al. (2024) (Table 2). The reconstructed $\delta^{18}O_{sw}$ data for all corals have been previously published (Ren et al., 2002; Wu et al., 2013; Todorović, Dissard, et al., 2024; Todorović, Wu, et al., 2024), but for the sake of using the same approach, monthly $\delta^{18}O_{sw}$ for Fiji 1F and Rarotonga 2R were recalculated using the parameters specified here. Two-tailed paired *t*-tests indicate that reconstructed $\delta^{18}O_{sw}$ means of Fiji and Rarotonga calculated with this method are not significantly different from the previously published data ($p < 0.0001$) and are highly correlated (2R, $r = 0.88$, 1F, $r = 0.99$, both at $p < 0.0001$).

2.4.1. Coral Proxy Indices

To facilitate the interpretation and use of the indices, we calculated both the proxy ($SPCZ_c$ $\delta^{18}O$, -Sr/Ca, -$\delta^{18}O_{sw}$) and, following the method of Linsley et al. (2008, 2015), the coral SST and SSS ($SPCZ_c$-SST, -SSS) indices.

To calculate the proxy composite indices, coral $\delta^{18}O$, Sr/Ca, and $\delta^{18}O_{sw}$ records from Rotuma (RO2), Fiji (1F), Tonga (TNI2), and Rarotonga (2R) were centered by removing the respective 145-year mean (1850–1995, the period spanning all the records). The average, standard deviation, and standard error were then calculated across all coral records for each month (Linsley et al., 2008, 2015).

Coral-based SPCZ indices of SST and SSS ($SPCZ_c$-SST, $SPCZ_c$-SSS) were calculated to explore relative SST and SSS changes in the region. Coral Sr/Ca time-series and reconstructed $\delta^{18}O_{sw}$ records were first regressed against local ERSST and D-SSS using the RMA method. The Sr/Ca-SST and $\delta^{18}O_{sw}$-SSS for each coral were then centered by removing the respective 145-year mean (1850–1995, the period spanning all the records). The resulting centered data were then averaged into indices, and variance and standard error (±s.e.) were calculated as described above.

2.5. Time Series and Statistical Analyses

Pearson product moment correlation (hereafter referred to as correlation) was used to determine the significance of relationships between all Sr/Ca and $\delta^{18}O_{sw}$ time series and the $SPCZ_c$ indices to their respective SST and SSS instrumental datasets (see Tables S2, S3, S4 in Supporting Information S1).

To explore significant spectra and variability, detrended $SPCZ_c$ indices were analyzed using Multitaper spectral analysis (MTM), with 3 tapers and an adaptive spectrum in PAST v4 (Hammer et al., 2001). Inter-annual (3–7.5 years) and low-pass (20-year, detrended) bands were filtered for all proxies, as well as the SPCZ Position index (SPCZi) based on normalized mean sea-level pressure difference between Apia, Samoa, and Suva, Fiji (Higgins et al., 2020; Salinger et al., 2014), and the Southern Oscillation Index (SOI). The Tripole Index for Interdecadal Pacific Oscillation (TPI) (Henley et al., 2015) is already a low-pass filtered index. The finite impulse response (FIR) filter in PASTv4 (Hammer et al., 2001) was used for this purpose with a 0.041–0.011 window size for the band-pass filter, and a 0.004 to 0 window size for the low-pass of detrended data. A high order of 255 and a narrow transition of 0.008 were used in both cases to achieve a filter with high frequency resolution and sharp distinction between frequencies. This filtering facilitated the isolation of major interannual (ENSO) and interdecadal (IPO) modes of variability, as recorded by the $SPCZ_c$ indices. For SPCZ zonal event reconstruction, $SPCZ_c$ $\delta^{18}O_{sw}$ and D-SSS were filtered to include some subannual variability and exclude lower frequency variability (10 months–7.5 years), due to the specific signature SPCZ zonal events

Table 3
Regression Equations of Composite SPCZ$_c$ Sr/Ca Against Composite ERSST (1854–1996, N = 1,715), and SPCZ$_c$ $\delta^{18}O_{sw}$ Against Composite D-SSS (1956–1996, N = 491)

SPCZ$_c$ Sr/Ca with ERSST 2° × 2°	R (r^2)	SPCZ$_c$ $\delta^{18}O_{sw}$ with D-SSS 1° × 1°	R (r^2)
Sr/Ca (mmol/mol) = −0.060 (±0.001) * SST (°C) + 1.6231 (±0.020)	−0.86 (0.73)	$\delta^{18}O_{sw}$ (‰) = 0.431 (±0.015) * SSS (S_p) – 0.0501 (±0.003)	0.64 (0.40)

Note. All significant at the $p < 0.0001$ level.

leave in the instrumental SSS data of the region, as discussed later in the text. Wavelet transform analysis was completed with PAST v4 (Hammer et al., 2001) to examine temporal changes in variability.

3. Results and Discussion

3.1. The SPCZ$_c$ Regional Indices

Reconstructing the long-term oceanographic variability of the SPCZ is key to better understanding its impacts on the Pacific climate system, as well as the effects of the changing climate on its complex dynamics. Previous multi-coral replication and composite studies realized the advantage of the compositing method in describing regional conditions while increasing the climatic signal-to-noise ratio (Dassié et al., 2014, 2018; DeLong et al., 2007; Linsley et al., 2008, 2015; Tierney et al., 2015). To construct an extended set of oceanographic variability indices to describe the SPCZ region, new high-resolution proxy records from Rotuma (RO2) and Tonga (TNI2) corals were joined to the existing coral-based reconstructions from Fiji and Rarotonga (1F, 2R) into new SPCZ$_c$ indices (Table 1, Figures 2a and 2b). Adding the Tonga TNI2 coral to the composite in place of TH1 extended the higher-resolution temporal coverage from 1944 (TH1) to 1848 (TNI2). The $\delta^{18}O$ and Sr/Ca records of the two Tonga corals are highly reproducible over their replication period (1944–2004) (Sr/Ca $r = 0.58$, $p < 0.001$; $\delta^{18}O$ $r = 0.66$, $p < 0.001$, Figure S2 in Supporting Information S1). Adding the Rotuma *Porites* sp. to the SPCZ$_c$ indices provided a crucial extension of the regional coverage further northwest into the SPCZ fresh/warm pool.

To quantify the impact of adding additional records from the fresh pool to the existing coral SPCZ network, we compared our indices to sets generated without the Rotuma coral (see Figure S3, Tables S3 and S4 in Supporting Information S1). This represented the FTR region that was previously described in the literature. The original annual FTR Sr/Ca-SST (Linsley et al., 2015) and annually interpolated SPCZ$_c$-SST indices show a high correlation with each other throughout the reconstruction ($r = 0.87$, $p < 0.0001$, 1848–1996, $N = 149$). Both records achieve strong correlations to their respective composite ERSST (1960–1996, FTR Sr/Ca-SST $r = 0.75$, annual SPCZ$_c$-SST $r = 0.73$, $p < 0.0001$, $N = 36$, Figures S3A and S3B in Supporting Information S1). Our monthly interpolated SPCZ$_c$ Sr/Ca shows a correlation of 0.92 in the 1960–1996 period, improving on the individual coral correlations ranging from −0.27 to −0.80 (Table S2 in Supporting Information S1), and a generally high correlation back to the beginning of the ERSST dataset in 1854 (Table 3, and Table S3 in Supporting Information S1).

The main improvement in expanding the geographical coverage of the SPCZ is seen in SPCZ$_c$ $\delta^{18}O_{sw}$ obtaining better correlation with the instrumental SSS in comparison to the regional reconstruction without the Rotuma fresh pool endmember (Table S4 in Supporting Information S1). The SPCZ$_c$ $\delta^{18}O_{sw}$ index is the first composite index reported for the SPCZ region that is directly related to regional SSS. The index shows a strong correlation with its respective regional SSS (SPCZ$_c$ $\delta^{18}O_{sw}$: $r = 0.64$; SPCZ$_c$-SSS: $r = 0.64$ all $p < 0.0001$, $N = 491$) and is stronger compared to any of the single coral to SSS correlations ranging from 0.31 to 0.58 (Table S2 in Supporting Information S1). The SPCZ$_c$ $\delta^{18}O_{sw}$ index explains 40% of the variability in salinity of the region (Table 3).

SPCZ$_c$ Sr/Ca index shows a warming of 0.91 ± 0.11°C spanning the composite record using a Sr/Ca-SST sensitivity of −0.06 mmol mol^{-1} per °C. This result agrees with the 0.9°C warming observed in the composite ERSST from 1854 to 1996, and findings from previous coral-based and reanalysis studies from this region (Folland et al., 2003; Wu et al., 2013).

The salinity proxy, SPCZ$_c$ $\delta^{18}O_{sw}$ index, exhibits good agreement with the D-SSS (Table S4 in Supporting Information S1, and Figure 2, Table 3), considering the dissimilarity between different instrumental SSS products even for the same location (Todorović, Wu, et al., 2024). In the calibration period (1956–1996), both D-SSS and

$SPCZ_c$-SSS show non-significant trends toward increased salinity (0.01–0.03 S_p). Starting in the 1880s, the long-term secular freshening trend spanning the composite record equates to a significant change of 0.36 ± 0.02 S_p using the reconstructed $\delta^{18}O_{sw}$-SSS sensitivity of 0.43 ($p < 0.0001$).

The coral compositing approach surpasses the value of single cores and previous composites (Table S2 in Supporting Information S1) in achieving a more representative reconstruction of the SPCZ SST and SSS variability. Individual corals are subject to localized environmental conditions and exhibit intercolony differences even on neighboring reefs (e.g., Cahyarini et al., 2008; Dassié et al., 2014; DeLong et al., 2011; Linsley et al., 2008; Pfeiffer et al., 2009; Sayani et al., 2019). Individual corals can also exhibit diagenetic alteration to various extents (Hendy et al., 2007) or can be impacted by vital effects (Alpert et al., 2016). Compositing multiple coral records enhances their common climatic signals and smooths out the noise resulting from individual core variabilities, thus improving the detection and characterization of climate changes (Evans et al., 2002; Tierney et al., 2015; Wilson et al., 2010). $SPCZ_c$-SSS fills the critical data gap in the limited spatial and temporal coverage of instrumental SSS datasets and provides the first overview of the long-term SPCZ SSS variability (Figure 2b).

3.2. ENSO Impacts on the SPCZ SST and SSS

After the seasonal cycle, ENSO-related changes in the SPCZ are the largest mode of variability (Brown et al., 2020; Trenberth, 1976). This is reflected in the MTM analysis results (see Figure S5A in Supporting Information S1) with highly significant (99%) peaks for annual variability in coral $\delta^{18}O$ and Sr/Ca values and followed by significant (95%) peaks in the ENSO frequency band of 2–7 years (Trenberth, 1976). Coral-reconstructed $\delta^{18}O_{sw}$ shows a highly significant spectral peak (99%) near 5-year. The annual cycle is the least powerful and significant mode for reconstructed $\delta^{18}O_{sw}$, which reflects the smaller seasonal SSS variability in this region. Previous studies report significant frequency peaks in the ENSO band in $\delta^{18}O$ records generated from corals in the SPCZ region (Dassié et al., 2018; Linsley et al., 2006, 2008), showing strong correlations of the SSS, salinity front displacements, and ENSO variability. There is a lack of focus on ENSO variability responses in other coral proxies or in the previous regional composites based on annually averaged data ($\delta^{18}O$-based FT IDPO, Linsley et al., 2008; Sr/Ca-based FTR, Linsley et al., 2015). One of the indices of ENSO variability is the Southern Oscillation Index (SOI), an index that measures the sea level pressure difference between Darwin and Tahiti (Figure 3e). These atmospheric changes are related to the SST anomalies associated with the ENSO warm and cool phases. The interannual band-pass filtered data of all $SPCZ_c$ indices show highly significant negative correlations with the SOI ($p < 0.0001$, Table 4) as well as other ENSO indices (see Table S5 in Supporting Information S1), suggesting responses of both SST and SSS to ENSO variability. During El Niño episodes (indicated by negative SOI), shifts toward higher $\delta^{18}O$ and Sr/Ca values are observed (see Figures 3a and 3b), indicating cooling and/or increasing surface salinity in the region. Attenuation of the freshening peak, or a shift toward more saline conditions in $\delta^{18}O_{sw}$ values indicates the displacement of the salinity front toward the northwest during an El Niño event and a freshening and displacement of the front toward the southeast during La Niña events (Figures 3c and 3d). Previous efforts to decipher the imprints of Eastern Pacific (EP) El Niño versus Central Pacific (CP) El Niño on Pacific-wide SST anomalies based on the coral $\delta^{18}O$ proxy predominantly (Freund et al., 2019) found higher amplitude SST anomalies during EP events in El Niño SST regions. Based on our composite proxy results, we don't observe an increase in El Niño frequency between 1850 and 1900, 1900 and 1950, or from 1950 onwards (9 ± 1 EN in each 50-year bin), but we do observe a shift toward lower anomalies since 1980 that could correspond to an increase in CP events observed by Freund et al. (2019). La Niña events happened more often during the 1850–1900 period compared to 1900–1950, or from 1950 onwards, including a notable event in 1880 with markedly positive SST anomalies (Figure 3b). The lower SSTs during El Niño episodes can be attributed to the weakening of easterly trade winds and eastward movement of warm water. They are recorded in our SST proxy as increases in Sr/Ca indicating cooling from 0.40°C to 0.80°C on average during El Niño events. The atmospheric convection front shifting northeastward closer to the equator leads to reduced precipitation in the study area and advection of more saline water from the westward flowing South Equatorial Current (SEC) resulting in an increase in SSS during El Niño episodes compared to the ENSO neutral state baseline (Folland et al., 2002). SSS in the modern mean climatological SPCZ area responds with ~0.50 S_p increase to EP El Niño events of 1982/83 and 1992/93 associated with the SPCZ zonal events discussed later in the text. These anomalies are 2–3 times higher than during more moderate, usually CP ones, such as the ones in 1977, 1988/89, 1990/91, and 1992–95 (Qi et al., 2019; Singh et al., 2011). Higher anomalies can also be observed in our SSS proxy during the EP events of 1982/83 and 1991/92 (Figure 3c), compared to more moderate events such as ones in 1976/77 and 1986/87 (+0.1–0.2 S_p) (Figure 3c). As SPCZ zonal events are commonly associated with EP

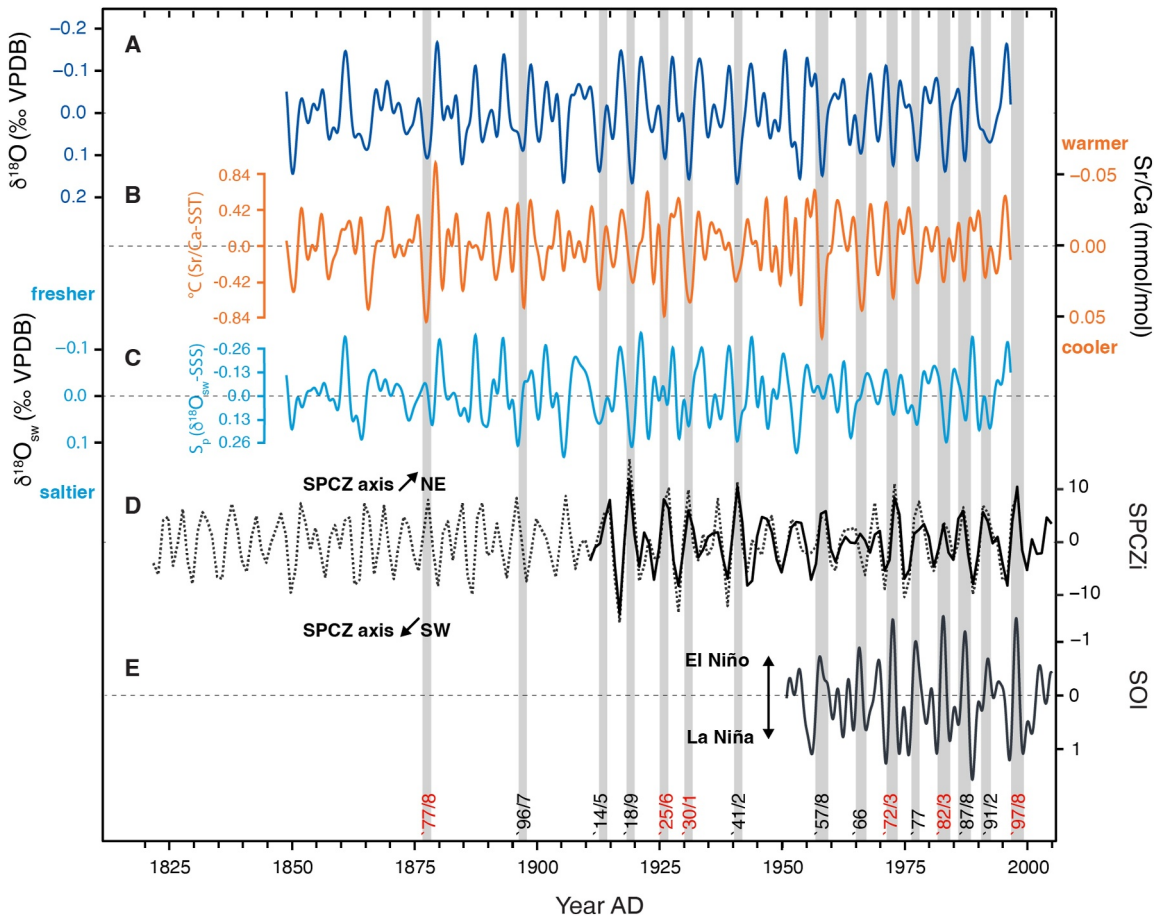

Figure 3. Interannual variability captured by the SPCZ$_c$ indices: (a) SPCZ$_c$ $\delta^{18}O$ band-pass; (b) SPCZ$_c$ Sr/Ca band-pass; and (c) SPCZ$_c$ $\delta^{18}O_{sw}$ band-pass, compared to the (d) SPCZi instrumental (solid black) and reconstructed (dotted). Positive values indicate shifts of the salinity front northeast, highly influenced by El Niño episodes, and negative values shifts toward southwest, usually during La Niña episodes. (e) SOI band-pass, where positive values indicate La Niña states, and negative ones El Niño states. Selected confirmed El Niño years (observed and reconstructed) are presented with shaded bands, with stronger episodes marked in red.

events, it is impossible to reliably reconstruct the measure of the EP versus CP anomalies in the region from this proxy alone. The same response to ENSO variability was also observed in the FTR region based on $\delta^{18}O$-SSS reconstruction, along with interannual salinity front displacements (Dassié et al., 2018). We observe multiple past episodes of increased salinity on a similar timescale, coinciding with Sr/Ca-SST cooling that could refer to past El Niño events (1896/97, 1906, 1918/19), or potentially past zonal events.

Table 4
Correlations of the Filtered SPCZ$_c$ Indices Against the Iinterannual and Interdecadal Variability Indices – ENSO (SOI, 1951–1996), SPCZ Movement (SPCZi Instr., 1911–1996), and IPO (Tripole Index – TPI, 1860–1996)

	SPCZ$_c$ $\delta^{18}O$	SPCZ$_c$-SST	SPCZ$_c$-SSS
SOI (band-pass)	−0.74, $p < 0.0001$	−0.65, $p < 0.0001$	−0.59, $p < 0.0001$
SPCZi instr. (band-pass)	0.63, $p < 0.0001$	−0.46, $p < 0.0001$	0.61, $p < 0.0001$
IPO (TPI) (low-pass)	0.33, $p < 0.0001$	−0.53, $p < 0.0001$	*−0.03, $p > 0.05$*
SPCZi instr. (low-pass)	*0.25, $p < 0.05$*	−0.47, $p < 0.0001$	*−0.03, $p > 0.05$*

Note. Correlations were calculated from band-pass and low-pass filtered data presented in Figures 3 and 5. Correlations with the significance of less than $p < 0.001$ in italic.

3.3. SPCZ Zonal Events Reconstruction

The SPCZ movement has been reconstructed with the SPCZi, an index based on evolving annual mean sea level pressure gradient between Fiji and Samoa back to 1910 (SPCZi instrumental, Salinger et al., 2014), with further extension to 700 CE using tree ring observations (SPCZi reconstructed, Higgins et al., 2020). All three $SPCZ_c$ proxies correlate significantly ($p < 0.0001$) with the SPCZi reconstructed, with $SPCZ_c$ $\delta^{18}O_{sw}$ being most useful as a predictor of the SPCZ position (Table 4). The variability of the SPCZ fresh pool, a large area of low SSS waters associated with the maximum precipitation axis, can be reconstructed with $\delta^{18}O_{sw}$ due to its strong correlation with SSS. When the SPCZi becomes more positive, it indicates an SPCZ shift to the northeast, adopting a more equatorial position. Concurrently, $SPCZ_c$ proxies exhibit positive anomalies when the SPCZi is positive, signifying increases in SSS and decreases in SST. Marked increases in salinity also correspond to the asymmetric or zonal events of the SPCZ (Vincent et al., 2011) (Figure 4b). During these events, the SPCZ central axis shifts almost parallel to and near the equator, as was observed in rainfall and SST instrumental data in 1982/3, 1991/2, and 1997/8 (Borlace et al., 2014; Cai et al., 2012) but is not captured by the SPCZi as it is an index of pressure between Samoa and Fiji (Higgins et al., 2020; Salinger et al., 2014).

There are no direct instrumental-based observations of SPCZ zonal events prior to 1979 but a coral-based $\delta^{18}O$-SSS reconstruction from the Makassar Strait in the Indonesian Throughflow (ITF) region provided evidence of truncated freshening or anomalous salinity regime changes and movement during confirmed zonal events (Linsley et al., 2017). Following the signature of anomalously higher salinity during normally low salinity fresh seasons, they generated a reconstruction of SPSZ zonal events dating back to 1740 CE. The salinity composite reconstruction from the SPCZ region has a markedly smaller seasonal cycle, yet spikes exceeding the typical annual SSS amplitude of 0.30 S_p (Gouriou & Delcroix, 2002) are evident during the zonal events of 1982/3, 1991/2, and 1997/98 (Figure 4d). Looking at the values exceeding the 95th percentile of the composite SSS band-pass data, another possible event in 1976/7 can be identified (Figure 4d).

The band-pass filtered $SPCZ_c$ $\delta^{18}O_{sw}$ record shows a robust relationship with the SSS composite (1956–1996), validating the timing of events ±1 year (Figure 4d), except for the event in 1991/2, that according to the SSS composite results, lasted only two months. The event of 1964/5 recorded in the $SPCZ_c$ $\delta^{18}O_{sw}$ is not reflected in the instrumental SSS, likely due to fewer observations prior to the 1970s (Delcroix et al., 2011). Anomalies in $\delta^{18}O_{sw}$ values exceeding the 95th percentile, conservatively set at 0.25 S_p, distinguish zonal events from the usual seasonal departure of 0.15 S_p from the average. Our results suggest that SPCZ zonal events are a phenomenon that has been occurring on a regular basis since at least the 1850s, approximately every 7 ± 3 years (Table S6 and Figure S4 in Supporting Information S1). A higher recurrence of the strongest SPCZ zonal events is observed in the early 1900s, coinciding with observed Pacific early twentieth-century surface air warming attributed to weakening trade winds (Thompson et al., 2015) (Figure S4 in Supporting Information S1). There is no clear increase in intensity of events throughout the reconstruction as shown by a non-significant Mann-Kendall test result, consistent with the findings of Linsley et al. (2017).

We identify 21 events in the 1848–1996 period, with the strongest ones coinciding with EP El Niño episodes (Figure 4c, and Table S6 in Supporting Information S1). By binning the reconstructed zonal events, seven episodes are observed from 1850 to 1900, nine episodes between 1900 and 1950 (see Figure S4 in Supporting Information S1), and five from 1950 to 2000, taking into account the events recognized in instrumental data. However, not all zonal events observed in this study from the SPCZ were identified from the Makassar Strait reconstruction. The Makassar Strait exhibits clear SSS annual cycles, where truncated fresh seasons can be easily identified, but the local oceanographic variability could also be affected separately by Indian Ocean Dipole (IOD), ENSO and Asian-Australian monsoon on the ITF currents network, water mixing and transport (Fallon & Guilderson, 2008; Guo et al., 2023; Meyers et al., 2007; Susanto et al., 2012). Thus, as the variability of SSS in the SPCZ is strongly impacted by the rainfall axis position (Figure 4d), it makes the region suited for zonal movement reconstructions without possible additional influence as observed in the ITF.

The zonal event in 1864/5 coincides with the stalagmite-recorded Vanuatu drought of 1865 ± 3 years (Partin et al., 2013) and the findings from the South Pacific drought atlas (Higgins et al., 2023). The event in 1873/4, the second strongest zonal event from our reconstruction that persisted for 7 months, preceded the Great Drought development from 1875 onwards that affected most of Asia, Brazil and Africa, and persisted fueled by the 1877/8 El Niño (falling just below our 95th percentile threshold) and a positive IOD (Davis, 2002; Singh et al., 2018). The EP El Niño events of the late nineteenth and beginning of the twentieth century (1904/5, 1918/9, 1986/7, 1983)

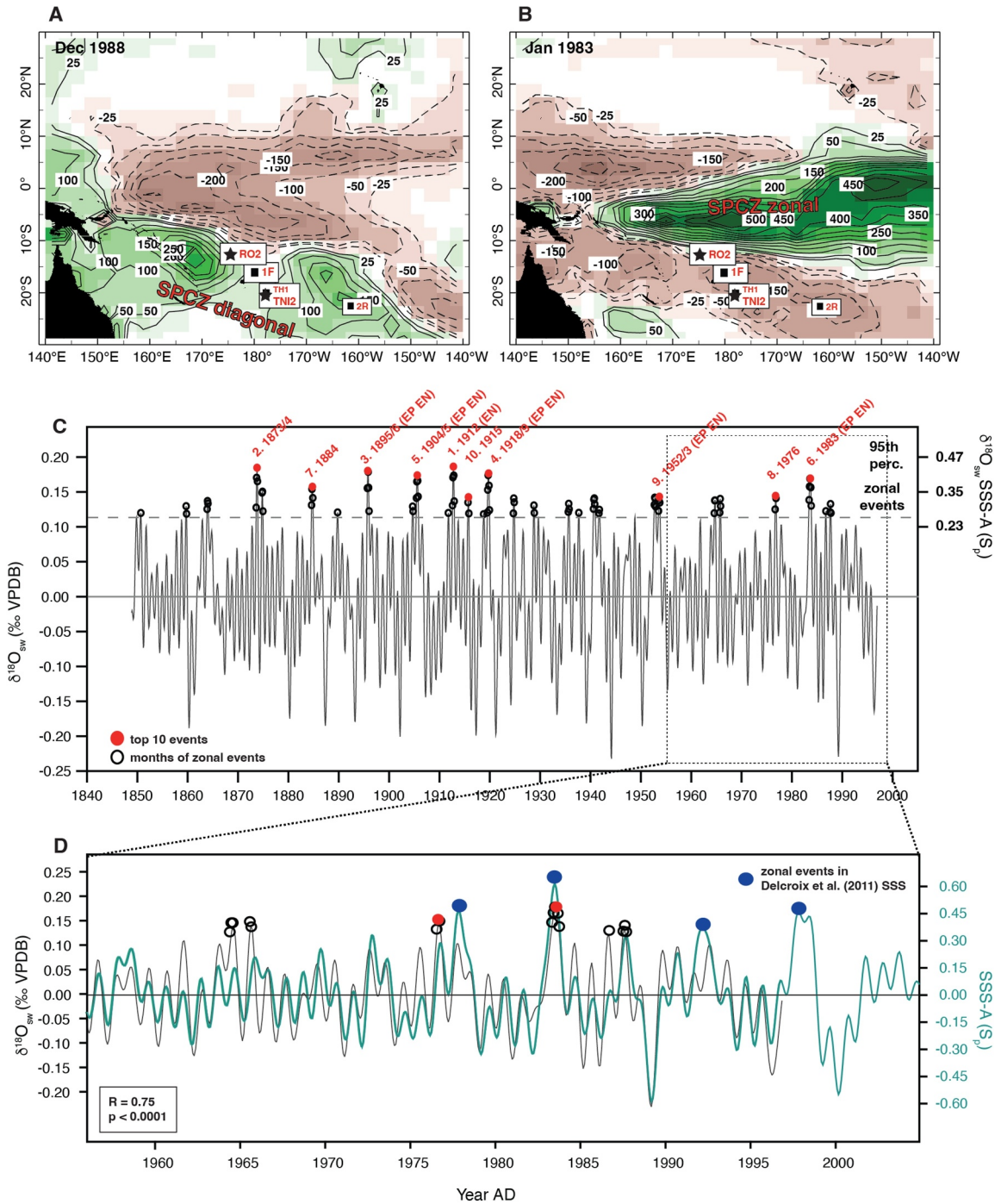

Figure 4. SPCZ zonal events validation and reconstruction: (a) SPCZ rainfall axis orientation for a baseline state; (b) and during a SPCZ zonal event. Gridded data plotted in both panels are monthly precipitation anomalies from CPC CAMS-OPI v0208 monthly gridded precipitation data set (Janowiak & Xie, 1999) using the LDEO Data Library viewer. Sampling locations of $SPCZ_c$ corals are depicted in both panels. (c) $SPCZ_c$ $\delta^{18}O_{sw}$ band-pass data with a 95th percentile cut off for identifying periods of anomalously higher salinity, indicating the SPCZ shift equatorward; (d) Band-pass Delcroix et al. (2011) SSS data (in practical salinity (S_p) units) and $SPCZ_c$ $\delta^{18}O_{sw}$ band-pass data correlate strongly in the overlapping period ($r = 0.78$ since 1970, when numbers of observations increase) and reveal a common response to reported zonal events.

produced some of the largest anomalies indicating zonal orientation and drier conditions in the SPCZ. While not all reconstructed zonal events agree between this study and previous findings (Higgins et al., 2023; Linsley et al., 2017), our highly resolved local network of corals does show periodicity and potential drivers that

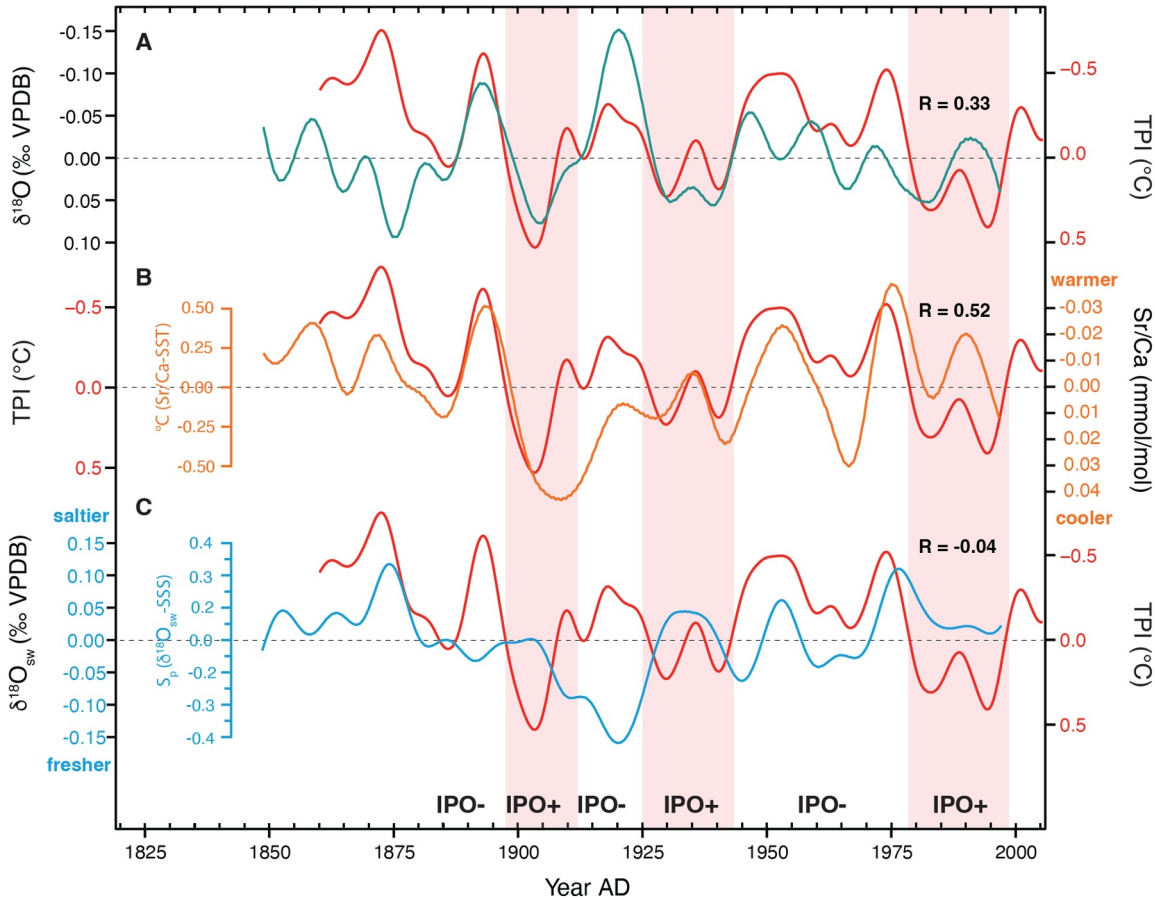

Figure 5. Low-frequency variability described by instrumental data and by low-pass filtered, detrended SPCZ$_c$ indices. (a) SPCZ$_c$ $\delta^{18}O$ compared to the Tripole Index (TPI, low-pass filtered, temperature anomaly, °C) as an index of IPO. (b) SPCZ$_c$ Sr/Ca compared to the low-pass filtered TPI. (c) $\delta^{18}O_{sw}$ compared to the low-pass filtered TPI. IPO positive phases are shaded in red. Correlations presented here are between the low-pass, detrended, coral proxy data ($\delta^{18}O$, Sr/Ca, $\delta^{18}O_{sw}$) and the TPI.

underscore the predictions of increased number of zonal events in the future due to continued warming (Borlace et al., 2014; Cai et al., 2012). These records undoubtedly allow extension of SPCZ rainfall axis extreme position shifts beyond the traditional instrumental era.

3.4. Interdecadal SPCZ Variability

IPO warm (positive) and cool (negative) phases have been shown to coincide with previous periods of both global accelerated warming (1976–2000) and hiatus periods (1945–1975), respectively (England et al., 2014; Meehl et al., 2013). Periods of positive IPO phases are associated with positive SST anomalies in the eastern equatorial Pacific, and conversely, negative ones in the central west South and North Pacific (Henley et al., 2015). Coral $\delta^{18}O$ reconstructions were previously shown to be a skillful proxy for the South Pacific IPO tripole region (F-T IDPO, Henley et al., 2015; Linsley et al., 2008).

Highly significant (99%) increases in low-frequency variability in all three SPCZ$_c$ proxies (see Figure S5A in Supporting Information S1) are present, indicating that the dominant variance in the records occurs over timescales of 20 or more years. Wavelet transform analysis shows consistently significant (see Figure S5B in Supporting Information S1, $p < 0.05$) decadal variability in the SPCZ$_c$ Sr/Ca index with a period between 15 and 30 years throughout the reconstruction, corresponding to IPO phase shift interval commonly found in the literature (Henley, 2017; Mantua & Hare, 2002; Parker et al., 2007). The degree of correlation between SPCZ$_c$ Sr/Ca and IPO is comparable to the previous Sr/Ca composite over the Fiji to Rarotonga region (FTR index, Linsley et al., 2015). SPCZ$_c$ Sr/Ca achieves a better reconstruction of past IPO phases (Table 4, Figure 5b) compared to $\delta^{18}O$ as an SST proxy, while providing a convenient means to quantify IPO associated anomalies in degrees

Celsius. It reveals negative SST anomalies of up to approximately 0.65°C during positive IPO phases and positive SST anomalies of up to around 0.75°C during negative IPO phases. A period of higher amplitude in $SPCZ_c$ $\delta^{18}O$ anomalies during 1890–1950 has been previously identified in regional corals (Bagnato et al., 2005). It coincides with decadal cooling observed in the $SPCZ_c$ Sr/Ca from 1900 to the 1940s, surface air warming, and trade wind weakening (Thompson et al., 2015). From the 1880s to the mid-1920s, there is a period of anomalous variability in the $SPCZ_c$ $\delta^{18}O_{sw}$ as well. The early 1900s show a lack of freshening during a positive IPO phase, potentially related to a period of droughts between 1878 and 1889 identified in the drought reconstruction of the South Pacific (Higgins et al., 2023) or SPCZ zonal events as identified in this work.

The periods of SST cooling in the SPCZ region are usually associated with increased surface salinity due to less precipitation and the advection of higher salinity central gyre water to the northwest. Lowpass filtered $SPCZ_c$-SSS and SST reconstructions exhibit a weak, negative correlation ($r = -0.12$, $p < 0.01$), indicating that evaporation and precipitation balance contribute little to the SPCZ upper water column salinity variability. Removing the linear trend from both results in a moderately strong, positive correlation ($r = 0.45$, $p < 0.0001$), implying increases in salinity coinciding with periods of warming. This positive correlation between detrended reconstructed SST and SSS is in line with the latest reconstructions of decadal salinity variability from observation and model data showing concurrent warming and salinification in the SPCZ region after the shift to a negative IPO phase in the 1990s (Li et al., 2019). A very weak correlation between $SPCZ_c$ $\delta^{18}O_{sw}$ and IPO ($r = -0.04$) leads us to believe that IPO might not play an important role in decadal salinity variability in the SPCZ directly, but the associated changes in wind-driven advection. With the intensification of the Pacific Walker circulation and trade winds, shallow Pacific subtropical-tropical overturning cells are enhanced. This results in saltier extratropical waters being subducted and upwelling in the low latitude equatorial band, thus increasing salinity in the Western Tropical Pacific, as observed during the last intensification of the Walker Circulation since the 1990s (Du et al., 2015).

There is a stronger prevalence of negative IPO phases in the last 600 years observed in tree ring reconstructions (Vance et al., 2022). In addition to the anomalously long negative IPO phase during 1945–1980s, the $SPCZ_c$ Sr/Ca shows another period of predominantly negative state from the 1850s to 1885. The increasing upper ocean heat content of the South Pacific observed in the decades since the 1950s (Levitus et al., 2012) coincided with a negative IPO phase. From 1992 to 2011, a transition period into another IPO negative phase has led to an irreversible heat gain in the subsurface western Pacific (Maher et al., 2018). The concurrent intensification of the ITF transport has furthermore led to increased heat transport from the western Pacific into the Indian Ocean. While the heat loss during neutral and positive IPO states would lead to some surface cooling, there is still a net increase in heat gain in the Indo-Pacific region (Maher et al., 2018). A shift toward a more negative IPO state would mean warming and continued salinification of the surface ocean in the SPCZ region. While it is unclear what this would mean for the SPCZ precipitation trends, it is imperative to decipher the contributing factors, as the ocean heat content in the southwestern Pacific is a major contributor to regional heat transport and subsurface warming (Cravatte et al., 2009; Maher et al., 2018; Roxy et al., 2019; Weller et al., 2016).

3.5. Summary

The SW Pacific is a region of extreme importance to the Pacific-wide and global climate patterns, and at the same time, particularly lacking in instrumental climate observations older than a few decades. The efforts to improve the understanding of large-scale temperature and hydrological variability in the Pacific Ocean are an ongoing project (PAGES Hydro2k Consortium, 2017; Walter et al., 2023). They underscore the importance of adding new, long coral-based reconstructions from various points in this region. Our study contributes new insights into the SPCZ long-term trends in SST and SSS, as well as their responses to past interannual and interdecadal forcing. The $SPCZ_c$ extended coral network encompasses four sites spatially positioned to capture the extent of the SPCZ axis. In regressions with instrumental data, SSS variability is still captured, but to a lesser extent than the SST. Considering that there is a scarcity of available in-situ SSS measurements from these locations to capture the extent of hydrological variability present, we consider this contribution a valuable insight into the relative SSS changes dating back 100 years more than the available data. Filtered $SPCZ_c$ indices show highly significant correlations with the Pacific indices of interannual and interdecadal variability and can effectively reconstruct past ENSO variability, SPCZ movement, and IPO phases. We present a first reconstruction of SPCZ zonal events from the region, complementing previous efforts in reconstructions from instrumental and coral data. We identify 21 events in the 1848–1996 period and notice an increase in frequency during warming periods. We show here

that $SPCZ_c$ low-pass filtered Sr/Ca can be a skillful proxy not only for TPI Region 3, but also for TPI in general. These results confirm the utility of coral-based climate reconstructions and their value in improving climate models for future forecasts (Greene et al., 2008; Huang et al., 2021).

Further work is needed to characterize effects of changes in ENSO variability and replicate the findings, such as reconstructing CP versus EP El Niño, or changes in their frequency. Similarly, centennial timescale changes still fall short of being captured by the corals due to the small number of records going back far enough for reliable composite indices. Understanding the climatic variability of this region is essential in the face of global climate change. Changes in the SPCZ affect climate patterns in the wider region, and understanding past variability can help build climate change resilience in the island nations of the South Pacific and their ecosystems.

Conflict of Interest

The authors declare no conflicts of interest relevant to this study.

Data Availability Statement

Open Access funding was enabled and organized by Project DEAL. Coral proxy composites ($SPCZ_c$ $\delta^{18}O$, Sr/Ca, $\delta^{18}O_{sw}$), and coral-based SST and SSS composites ($SPCZ_c$ Sr/Ca-SST, $\delta^{18}O_{sw}$-SSS) and their standard errors have been deposited at the PANGAEA Repository (Data Publisher for Earth and Environmental Science), at Todorović et al. (2025).

Coral proxy data used for calculating the composite indices has been obtained from the PANGAEA Repository (Todorović, Dissard, et al., 2024), originally published in Todorović, Wu, et al. (2024), and from the original publications' authors (Linsley et al., 2000, 2004, 2008).

The ERSST data set (Huang et al., 2015) is publicly available and was obtained from the IRI/LDEO Climate Data Library (http://iridl.ldeo.columbia.edu/SOURCES/.NOAA/.NCDC/.ERSST/index.html, accessed 28 May 2020).

The Southwest Pacific gridded instrumental SSS data used in this study is publicly available through the Sedoo repository (Delcroix et al., 2011; accessed 1 August 2022).

South Pacific Convergence Zone Position indices (SPCZi) (Higgins et al., 2020; Salinger et al., 2014) are publicly available (https://www.ncei.noaa.gov/pub/data/paleo/treering/reconstructions/higgins2020spczi.txt, accessed 17 April 2023).

The Southern Oscillation Index (SOI) is publicly available (https://www.cpc.ncep.noaa.gov/data/indices/soi, accessed 18 June 2022).

Tripole Index for Interdecadal Pacific Oscillation (TPI) (Henley et al., 2015) is publicly available (https://psl.noaa.gov/data/timeseries/IPOTPI/, accessed 17 April 2023).

Acknowledgments
We thank Marie Harbott for her constructive comments on the manuscript. The OASIS project was funded by the Federal Ministry of Education and Research (BMBF) under the "Make Our Planet Great Again – German Research Initiative", 57429626 to Dr. Henry C. Wu (Junior Research Group Leader), implemented by the German Academic Exchange Service (DAAD). Partial funding was provided to Braddock K. Linsley by the Vetlesen Foundation via a gift to the Lamont-Doherty Earth Observatory. Open Access funding enabled and organized by Projekt DEAL.

References

Alpert, A. E., Cohen, A. L., Oppo, D. W., DeCarlo, T. M., Gove, J. M., & Young, C. W. (2016). Comparison of equatorial Pacific sea surface temperature variability and trends with Sr/Ca records from multiple corals. *Paleoceanography*, *31*(2), 252–265. https://doi.org/10.1002/2015PA002897

Bagnato, S., Linsley, B. K., Howe, S. S., Wellington, G. M., & Salinger, J. (2005). Coral oxygen isotope records of interdecadal climate variations in the South Pacific Convergence Zone region. *Geochemistry, Geophysics, and Geosystems*, *6*. https://doi.org/10.1029/2004GC000879

Baxter, I., Ding, Q., Schweiger, A., L'Heureux, M., Baxter, S., Wang, T., et al. (2019). How tropical Pacific surface cooling contributed to accelerated sea ice melt from 2007 to 2012 as ice is thinned by anthropogenic forcing. *Journal of Climate*, *32*(24), 8583–8602. https://doi.org/10.1175/JCLI-D-18-0783.1

Bonan, D. B., & Blanchard-Wrigglesworth, E. (2020). Nonstationary teleconnection between the Pacific Ocean and Arctic sea ice. *Geophysical Research Letters*, *47*(2), e2019GL085666. https://doi.org/10.1029/2019GL085666

Borlace, S., Santoso, A., Cai, W., & Collins, M. (2014). Extreme swings of the South Pacific Convergence Zone and the different types of El Niño events. *Geophysical Research Letters*, *41*(13), 4695–4703. https://doi.org/10.1002/2014GL060551

Brown, J. R., Lengaigne, M., Lintner, B. R., Widlansky, M. J., Van Der Wiel, K., Dutheil, C., et al. (2020). South Pacific Convergence Zone dynamics, variability and impacts in a changing climate. *Nature Reviews Earth & Environment*, *1*(10), 530–543. https://doi.org/10.1038/s43017-020-0078-2

Cahyarini, S. Y., Pfeiffer, M., Timm, O., Dullo, W.-C., & Schönberg, D. G. (2008). Reconstructing seawater $\delta^{18}O$ from paired coral $\delta^{18}O$ and Sr/Ca ratios: Methods, error analysis and problems, with examples from Tahiti (French Polynesia) and Timor (Indonesia). *Geochimica et Cosmochimica Acta*, *72*(12), 2841–2853. https://doi.org/10.1016/j.gca.2008.04.005

Cai, W., Lengaigne, M., Borlace, S., Collins, M., Cowan, T., McPhaden, M. J., et al. (2012). More extreme swings of the South Pacific Convergence Zone due to greenhouse warming. *Nature*, *488*(7411), 365–369. https://doi.org/10.1038/nature11358

Chen, G., Fang, C., Zhang, C., & Chen, Y. (2004). Observing the coupling effect between warm pool and "rain pool" in the Pacific Ocean. *Remote Sensing of Environment*, *91*, 153–159. https://doi.org/10.1016/j.rse.2004.02.010

Clem, K. R., Lintner, B. R., Broccoli, A. J., & Miller, J. R. (2019). Role of the South Pacific Convergence Zone in West Antarctic decadal climate variability. *Geophysical Research Letters*, *46*(12), 6900–6909. https://doi.org/10.1029/2019GL082108

Corrège, T. (2006). Sea surface temperature and salinity reconstruction from coral geochemical tracers. *Palaeogeography, Palaeoclimatology, Palaeoecology*, *232*(2–4), 408–428. https://doi.org/10.1016/j.palaeo.2005.10.014

Cravatte, S., Delcroix, T., Zhang, D., McPhaden, M., & Leloup, J. (2009). Observed freshening and warming of the western Pacific warm pool. *Climate Dynamics*, *33*(4), 565–589. https://doi.org/10.1007/s00382-009-0526-7

Dassié, E. P., Hasson, A., Khodri, M., Lebas, N., & Linsley, B. K. (2018). Spatiotemporal variability of the South Pacific Convergence Zone fresh pool eastern front from coral-derived surface salinity data. *Journal of Climate*, *31*(8), 3265–3288. https://doi.org/10.1175/JCLI-D-17-0071.1

Dassié, E. P., Linsley, B. K., Corrège, T., Wu, H. C., Lemley, G. M., Howe, S., & Cabioch, G. (2014). A Fiji multi-coral $\delta^{18}O$ composite approach to obtaining a more accurate reconstruction of the last two-centuries of the ocean-climate variability in the South Pacific Convergence Zone region. *Paleoceanography*, *29*(12), 1196–1213. https://doi.org/10.1002/2013PA002591

Davis, M. (2002). *Late Victorian holocausts: El Niño famines and the making of the third world*. Verso Books.

Davis, R. E., Talley, L. D., Roemmich, D., Owens, W. B., Rudnick, D. L., Toole, J., et al. (2019). 100 Years of Progress in ocean observing systems. *Meteorological Monographs*, *59*, 3.1–3.3. https://doi.org/10.1175/AMSMONOGRAPHS-D-18-0014.1

DeCarlo, T. M., Gaetani, G. A., Cohen, A. L., Foster, G. L., Alpert, A. E., & Stewart, J. A. (2016). Coral Sr-U thermometry. *Paleoceanography*, *31*(6), 626–638. https://doi.org/10.1002/2015PA002908

Delcroix, T., Alory, G., & Cravatte, S. (2011). A gridded sea surface salinity data set for the Pacific Ocean. [Dataset]. *Odatis*. https://doi.org/10.6096/SSS-LEGOS-GRID-PAC

Delcroix, T., Henin, C., Porte, V., & Arkin, P. (1996). Precipitation and sea-surface salinity in the tropical Pacific Ocean. *Deep-Sea Research Part A Oceanographic Research Papers*, *43*(7), 1123–1141. https://doi.org/10.1016/0967-0637(96)00048-9

DeLong, K. L., Flannery, J. A., Maupin, C. R., Poore, R. Z., & Quinn, T. M. (2011). A coral Sr/Ca calibration and replication study of two massive corals from the Gulf of Mexico. *Palaeogeography, Palaeoclimatology, Palaeoecology*, *307*(1–4), 117–128. https://doi.org/10.1016/j.palaeo.2011.05.005

DeLong, K. L., Quinn, T. M., & Taylor, F. W. (2007). Reconstructing twentieth-century Sea surface temperature variability in the southwest Pacific: A replication study using multiple coral Sr/Ca records from New Caledonia. *Paleoceanography*, *22*(4). https://doi.org/10.1029/2007PA001444

D'Olivo, J. P., Sinclair, D. J., Rankenburg, K., & McCulloch, M. T. (2018). A universal multi-trace element calibration for reconstructing sea surface temperatures from long-lived Porites corals: Removing 'vital-effects'. *Geochimica et Cosmochimica Acta*, *239*, 109–135. https://doi.org/10.1016/j.gca.2018.07.035

Du, Y., Zhang, Y., Feng, M., Wang, T., Zhang, N., & Wijffels, S. (2015). Decadal trends of the upper ocean salinity in the tropical Indo-Pacific since mid-1990s. *Scientific Reports*, *5*(1), 16050. https://doi.org/10.1038/srep16050

England, M. H., McGregor, S., Spence, P., Meehl, G. A., Timmermann, A., Cai, W., et al. (2014). Recent intensification of wind-driven circulation in the Pacific and the ongoing warming hiatus. *Nature Climate Change*, *4*(3), 222–227. https://doi.org/10.1038/nclimate2106

Evans, M. N., Kaplan, A., & Cane, M. A. (2002). Pacific sea surface temperature field reconstruction from coral $\delta^{18}O$ data using reduced space objective analysis. *Paleoceanography*, *17*, 7-1–7-13. https://doi.org/10.1029/2000PA000590

Fairbanks, R. G., Evans, M. N., Rubenstone, J. L., Mortlock, R. A., Broad, K., Moore, M. D., & Charles, C. D. (1997). Evaluating climate indices and their geochemical proxies measured in corals. *Coral Reefs*, *16*(5), S93–S100. https://doi.org/10.1007/s003380050245

Fallon, S. J., & Guilderson, T. P. (2008). Surface water processes in the Indonesian throughflow as documented by a high-resolution coral $\Delta^{14}C$ record. *Journal of Geophysical Research*, *113*(C9). https://doi.org/10.1029/2008JC004722

Folland, C., Salinger, M., Jiang, N., & Rayner, N. (2003). Trends and variations in South Pacific island and ocean surface temperatures. *Journal of Climate*, *16*(17), 2859–2874. https://doi.org/10.1175/1520-0442(2003)016<2859:TAVISP>2.0.CO;2

Folland, C. K., Renwick, J. A., Salinger, M. J., & Mullan, A. B. (2002). Relative influences of the interdecadal Pacific oscillation and ENSO on the South Pacific Convergence Zone. *Geophysical Research Letters*, *29*(13), 21-1–21-4. https://doi.org/10.1029/2001GL014201

Freund, M. B., Henley, B. J., Karoly, D. J., McGregor, H. V., Abram, N. J., & Dommenget, D. (2019). Higher frequency of Central Pacific El Niño events in recent decades relative to past centuries. *Nature Geoscience*, *12*(6), 450–455. https://doi.org/10.1038/s41561-019-0353-3

Gaetani, G. A., & Cohen, A. L. (2006). Element partitioning during precipitation of aragonite from seawater: A framework for understanding paleoproxies. *Geochimica et Cosmochimica Acta*, *70*(18), 4617–4634. https://doi.org/10.1016/j.gca.2006.07.008

Gouriou, Y., & Delcroix, T. (2002). Seasonal and ENSO variations of sea surface salinity and temperature in the South Pacific Convergence Zone during 1976-2000. *Journal of Geophysical Research*, *107*, SRF121–SRF1214. https://doi.org/10.1029/2001JC000830

Greene, J. S., Klatt, M., Morrissey, M., & Postawko, S. (2008). The comprehensive Pacific rainfall database. *Journal of Atmospheric Ocean Technology*, *25*(1), 71–82. https://doi.org/10.1175/2007JTECHA904.1

Guo, Y., Li, Y., Cheng, L., Chen, G., Liu, Q., Tian, T., et al. (2023). An updated estimate of the Indonesian throughflow geostrophic transport: Interannual variability and salinity effect. *Geophysical Research Letters*, *50*(13), e2023GL103748. https://doi.org/10.1029/2023GL103748

Hammer, O., Harper, D. A. T., & Ryan, P. D. (2001). PAST: Paleontological statistics Software package for education and data analysis [Software]. *Paleontology Electronics*, *4*, 9.

Hendy, E. J., Gagan, M. K., Lough, J. M., McCulloch, M., & De Menocal, P. B. (2007). Impact of skeletal dissolution and secondary aragonite on trace element and isotopic climate proxies in *Porites* corals. *Paleoceanography*, *22*(4), n/a-n–a. https://doi.org/10.1029/2007PA001462

Henley, B. J. (2017). Pacific decadal climate variability: Indices, patterns and tropical-extratropical interactions. *Global Planetary Change*, *155*, 42–55. https://doi.org/10.1016/j.gloplacha.2017.06.004

Henley, B. J., Gergis, J., Karoly, D. J., Power, S., Kennedy, J., & Folland, C. K. (2015). A tripole index for the interdecadal Pacific oscillation. *Climate Dynamics*, *45*(11–12), 3077–3090. https://doi.org/10.1007/s00382-015-2525-1

Higgins, P. A., Palmer, J. G., Andersen, M. S., Turney, C. S. M., & Johnson, F. (2023). Extreme events in the multi-proxy South Pacific drought atlas. *Climate Change*, *176*(8), 105. https://doi.org/10.1007/s10584-023-03585-2

Higgins, P. A., Palmer, J. G., Turney, C. S. M., Andersen, M. S., & Cook, E. R. (2020). One thousand three hundred years of variability in the position of the South Pacific Convergence Zone. *Geophysical Research Letters*, *47*(17), e2020GL088238. https://doi.org/10.1029/2020GL088238

Huang, B., Banzon, V., Freeman, J., Lawrimore, J., Liu, W., Peterson, T., et al. (2015). Extended reconstructed Sea Surface temperature version 4 (ERSST.v4). Part I: Upgrades and Intercomparisons. *Journal of Climate*, *28*(3), 911–930. https://doi.org/10.1175/JCLI-D-14-00006.1

Huang, B., Liu, C., Banzon, V., Freeman, E., Graham, G., Hankins, B., et al. (2021). Improvements of the daily optimum interpolation Sea Surface temperature (DOISST) version 2.1. *Journal of Climate*, *34*(8), 2923–2939. https://doi.org/10.1175/JCLI-D-20-0166.1

Huang, B., Liu, C., Ren, G., Zhang, H.-M., & Zhang, L. (2019). The role of Buoy and Argo observations in two SST analyses in the global and tropical Pacific Oceans. *Journal of Climate*, *32*(9), 2517–2535. https://doi.org/10.1175/JCLI-D-18-0368.1

Janowiak, J. E., & Xie, P. (1999). CAMS–OPI: A global satellite–rain Gauge merged product for real-time precipitation monitoring applications. *Journal of Climate*, *12*(11), 3335–3342. https://doi.org/10.1175/1520-0442(1999)012<3335:COAGSR>2.0.CO;2

LeGrande, A. N., & Schmidt, G. A. (2006). Global gridded data set of the oxygen isotopic composition in seawater. *Geophysical Research Letters*, *33*(12). https://doi.org/10.1029/2006GL026011

Levitus, S., Antonov, J. I., Boyer, T. P., Baranova, O. K., Garcia, H. E., Locarnini, R. A., et al. (2012). World ocean heat content and thermosteric sea level change (0-2000 m), 1955-2010: World Ocean Heat Content. *Geophysical Research Letters*, *39*(10). https://doi.org/10.1029/2012GL051106

Li, G., Zhang, Y., Xiao, J., Song, X., Abraham, J., Cheng, L., & Zhu, J. (2019). Examining the salinity change in the upper Pacific Ocean during the Argo period. *Climate Dynamics*, *53*(9–10), 6055–6074. https://doi.org/10.1007/s00382-019-04912-z

Linsley, B. K., Kaplan, A., Gouriou, Y., Salinger, J., De Menocal, P. B., Wellington, G. M., & Howe, S. S. (2006). Tracking the extent of the South Pacific Convergence Zone since the early 1600s. *Geochemistry, Geophysics, and Geosystems*, *7*(5). https://doi.org/10.1029/2005GC001115

Linsley, B. K., Wellington, G. M., & Schrag, D. P. (2000). Decadal sea surface temperature variability in the subtropical South Pacific from 1726 to 1997 A.D. *Science*, *290*(5494), 1145–1148. https://doi.org/10.1126/science.290.5494.1145

Linsley, B. K., Wellington, G. M., Schrag, D. P., Ren, L., Salinger, M. J., & Tudhope, A. W. (2004). Geochemical evidence from corals for changes in the amplitude and spatial pattern of South Pacific interdecadal climate variability over the last 300 years. *Climate Dynamics*, *22*, 1–11. https://doi.org/10.1007/s00382-003-0364-y

Linsley, B. K., Wu, H. C., Dassié, E. P., & Schrag, D. P. (2015). Decadal changes in South Pacific sea surface temperatures and the relationship to the Pacific decadal oscillation and upper ocean heat content. *Geophysical Research Letters*, *42*, 2358–2366. https://doi.org/10.1002/2015GL063045

Linsley, B. K., Wu, H. C., Rixen, T., Charles, C. D., Gordon, A. L., & Moore, M. D. (2017). SPCZ zonal events and downstream influence on surface ocean conditions in the Indonesian Throughflow region. *Geophysical Research Letters*, *44*(1), 293–303. https://doi.org/10.1002/2016GL070985

Linsley, B. K., Zhang, P., Kaplan, A., Howe, S. S., & Wellington, G. M. (2008). Interdecadal-decadal climate variability from multicoral oxygen isotope records in the South Pacific Convergence Zone region since 1650 A.D. *Paleoceanography*, *23*(2). https://doi.org/10.1029/2007PA001539

Lorrey, A., Dalu, G., Renwick, J., Diamond, H., & Gaetani, M. (2012). Reconstructing the South Pacific convergence zone position during the Presatellite era: A La Niña case study. *Monthly Weather Review*, *140*(11), 3653–3668. https://doi.org/10.1175/MWR-D-11-00228.1

Maher, N., England, M. H., Gupta, A. S., & Spence, P. (2018). Role of Pacific trade winds in driving ocean temperatures during the recent slowdown and projections under a wind trend reversal. *Climate Dynamics*, *51*(1–2), 321–336. https://doi.org/10.1007/s00382-017-3923-3

Mantua, N. J., & Hare, S. R. (2002). The Pacific decadal oscillation. *Journal of Oceanography*, *58*(1), 35–44. https://doi.org/10.1023/A:1015820616384

Matthews, A. J. (2012). A multiscale framework for the origin and variability of the South Pacific Convergence Zone. *Quarterly Journal of the Royal Meteorological Society*, *138*(666), 1165–1178. https://doi.org/10.1002/qj.1870

Meehl, G. A., Hu, A., Arblaster, J. M., Fasullo, J., & Trenberth, K. E. (2013). Externally forced and internally generated decadal climate variability associated with the interdecadal Pacific oscillation. *Journal of Climate*, *26*(18), 7298–7310. https://doi.org/10.1175/JCLI-D-12-00548.1

Menkes, C. E., Lengaigne, M., Marchesiello, P., Jourdain, N. C., Vincent, E. M., Lefèvre, J., et al. (2012). Comparison of tropical cyclogenesis indices on seasonal to interannual timescales. *Climate Dynamics*, *38*(1–2), 301–321. https://doi.org/10.1007/s00382-011-1126-x

Meyers, G., McIntosh, P., Pigot, L., & Pook, M. (2007). The years of El Niño, La Niña, and interactions with the tropical Indian Ocean. *Journal of Climate*, *20*(13), 2872–2880. https://doi.org/10.1175/JCLI4152.1

Montagna, P., McCulloch, M., Douville, E., López Correa, M., Trotter, J., Rodolfo-Metalpa, D., et al. (2014). Li/Mg systematics in scleractinian corals: Calibration of the thermometer. *Geochim. Cosmochim. Acta*, *132*, 288–310. https://doi.org/10.1016/j.gca.2014.02.005

Newman, M., Alexander, M. A., Ault, T. R., Cobb, K. M., Deser, C., Lorenzo, E. D., et al. (2016). The Pacific decadal oscillation, revisited. *Journal of Climate*, *29*(12), 4399–4427. https://doi.org/10.1175/JCLI-D-15-0508.1

PAGES Hydro2k Consortium. (2017). Comparing proxy and model estimates of hydroclimate variability and change over the Common Era. *Climate of the Past*, *13*(12), 1851–1900. https://doi.org/10.5194/cp-13-1851-2017

Parker, D., Folland, C., Scaife, A., Knight, J., Colman, A., Baines, P., & Dong, B. (2007). Decadal to multidecadal variability and the climate change background. *Journal of Geophysical Research*, *112*(D18), D18115. https://doi.org/10.1029/2007JD008411

Partin, J. W., Quinn, T. M., Shen, C.-C., Emile-Geay, J., Taylor, F. W., Maupin, C. R., et al. (2013). Multidecadal rainfall variability in South Pacific Convergence Zone as revealed by stalagmite geochemistry. *Geology*, *41*(11), 1143–1146. https://doi.org/10.1130/G34718.1

Pfeiffer, M., Dullo, W.-C., Dullo, W.-C., Zinke, J., & Garbe-Schönberg, C.-D. (2009). Three monthly coral Sr/Ca records from the Chagos Archipelago covering the period of 1950–1995 A.D.: Reproducibility and implications for quantitative reconstructions of sea surface temperature variations. *International Journal of Earth Sciences*, *98*(1), 53–66. https://doi.org/10.1007/s00531-008-0326-z

Porter, S. E., Mosley-Thompson, E., Thompson, L. G., & Wilson, A. B. (2021). Reconstructing an interdecadal Pacific oscillation index from a Pacific Basin–wide Collection of ice core records. *Journal of Climate*, *34*(10), 3839–3852. https://doi.org/10.1175/JCLI-D-20-0455.1

Power, S., Casey, T., Folland, C., Colman, A., & Mehta, V. (1999). Inter-decadal modulation of the impact of ENSO on Australia. *Climate Dynamics*, *15*(5), 319–324. https://doi.org/10.1007/s003820050284

Qi, J., Zhang, L., Qu, T., Yin, B., Xu, Z., Yang, D., et al. (2019). Salinity variability in the tropical Pacific during the central-Pacific and eastern-Pacific El Niño events. *Journal of Marine Systems*, *199*, 103225. https://doi.org/10.1016/j.jmarsys.2019.103225

Quinn, T. M., Taylor, F. W., Crowley, T. J., & Link, S. M. (1996). Evaluation of sampling resolution in coral stable isotope records: A case study using records from New Caledonia and Tarawa. *Paleoceanography*, *11*(5), 529–542. https://doi.org/10.1029/96pa01859

Ren, L., Linsley, B. K., Wellington, G. M., Schrag, D. P., & Hoegh-Guldberg, O. (2002). Deconvolving the $\delta^{18}O$ seawater component from subseasonal coral $\delta^{18}O$ and Sr/Ca at Rarotonga in the southwestern subtropical Pacific for the period 1726 to 1997 13.

Roxy, M. K., Dasgupta, P., McPhaden, M. J., Suematsu, T., Zhang, C., & Kim, D. (2019). Twofold expansion of the Indo-Pacific warm pool warps the MJO life cycle. *Nature*, *575*(7784), 647–651. https://doi.org/10.1038/s41586-019-1764-4

Salinger, M. J., McGree, S., Beucher, F., Power, S. B., & Delage, F. (2014). A new index for variations in the position of the South Pacific Convergence Zone 1910/11–2011/2012. *Climate Dynamics*, *43*(3–4), 881–892. https://doi.org/10.1007/s00382-013-2035-y

Sayani, H. R., Cobb, K. M., DeLong, K., Hitt, N. T., & Druffel, E. R. M. (2019). Intercolony $\delta^{18}O$ and Sr/Ca variability among *Porites* spp. corals at Palmyra Atoll: Toward more robust coral-based estimates of climate. *Geochemistry, Geophysics, and Geosystems*, *20*(11), 5270–5284. https://doi.org/10.1029/2019GC008420

Sinclair, D. J., Williams, B., & Risk, M. (2006). A biological origin for climate signals in corals—Trace element "vital effects" are ubiquitous in scleractinian coral skeletons. *Geophysical Research Letters*, *33*(17), L17707. https://doi.org/10.1029/2006GL027183

Singh, A., Delcroix, T., & Cravatte, S. (2011). Contrasting the flavors of El Niño-Southern Oscillation using sea surface salinity observations. *Journal of Geophysical Research*, *116*(C6), C06016. https://doi.org/10.1029/2010JC006862

Singh, D., Seager, R., Cook, B. I., Cane, M., Ting, M., Cook, E., & Davis, M. (2018). Climate and the global Famine of 1876–78. *Journal of Climate*, *31*(23), 9445–9467. https://doi.org/10.1175/JCLI-D-18-0159.1

Susanto, R. D., Ffield, A., Gordon, A. L., & Adi, T. R. (2012). Variability of Indonesian throughflow within Makassar Strait, 2004–2009. *Journal of Geophysical Research*, *117*(C9). https://doi.org/10.1029/2012JC008096

Tangri, N., Dunbar, R. B., Linsley, B. K., & Mucciarone, D. M. (2018). ENSO's Shrinking twentieth-century Footprint revealed in a Half-Millennium coral core from the South Pacific Convergence Zone. *Paleoceanography and Paleoclimatology*, *33*(11), 1136–1150. https://doi.org/10.1029/2017PA003310

Thompson, D. M., Cole, J. E., Shen, G. T., Tudhope, A. W., & Meehl, G. A. (2015). Early twentieth-century warming linked to tropical Pacific wind strength. *Nature Geoscience*, *8*(2), 117–121. https://doi.org/10.1038/ngeo2321

Thompson, D. M., Conroy, J. L., Konecky, B. L., Stevenson, S., DeLong, K. L., McKay, N., et al. (2022). Identifying hydro-sensitive coral $\delta^{18}O$ records for improved high-resolution temperature and salinity reconstructions. *Geophysical Research Letters*, *49*(9). https://doi.org/10.1029/2021GL096153

Tierney, J. E., Abram, N. J., Anchukaitis, K. J., Evans, M. N., Giry, C., Kilbourne, K. H., et al. (2015). Tropical sea surface temperatures for the past four centuries reconstructed from coral archives. *Paleoceanography*, *30*(3), 226–252. https://doi.org/10.1002/2014PA002717

Todorović, S., Dissard, D., Linsley, B. K., Kuhnert, H., & Wu, H. C. (2024). Paired $\delta^{18}O$ and Sr/Ca, and reconstructed $\delta^{18}O_{sw}$ records of *Porites* sp. from Rotuma (RO2) and Tonga (TNI2), Southwest Pacific [Dataset]. *PANGAEA*. https://doi.org/10.1594/PANGAEA.965772

Todorović, S., Linsley, B. K., Dissard, D., & Wu, H. C. (2025). Coral-based composite indices of sea surface temperature and salinity variability of the South Pacific Convergence Zone since 1848 [Dataset]. *PANGAEA*. https://doi.org/10.1594/PANGAEA.971484

Todorović, S., Wu, H. C., Linsley, B. K., Kuhnert, H., Menkes, C., Isbjakowa, A., & Dissard, D. (2024). Western Pacific warm pool warming and salinity front expansion since 1821 reconstructed from paired coral $\delta^{18}O$, Sr/Ca, and reconstructed $\delta^{18}O_{sw}$. *Paleoceanography and Paleoclimatology*, *39*(12), e2024PA004843. https://doi.org/10.1029/2024PA004843

Trenberth, K. E. (1976). Spatial and temporal variations of the Southern Oscillation. *Quarterly Journal of the Royal Meteorological Society*, *102*(433), 639–653. https://doi.org/10.1002/qj.49710243310

Vance, T. R., Kiem, A. S., Jong, L. M., Roberts, J. L., Plummer, C. T., Moy, A. D., et al. (2022). Pacific decadal variability over the last 2000 years and implications for climatic risk. *Communications Earth & Environment*, *3*, 1–9. https://doi.org/10.1038/s43247-022-00359-z

Vautard, R., & Ghil, M. (1989). Singular spectrum analysis in nonlinear dynamics, with applications to paleoclimatic time series. *Physica D: Nonlinear Phenomena*, *35*(3), 395–424. https://doi.org/10.1016/0167-2789(89)90077-8

Vincent, D. G. (1994). The South Pacific convergence zone (SPCZ): A review. *Monthly Weather Review*, *122*(9), 1949–1970. https://doi.org/10.1175/1520-0493(1994)122<1949:TSPCZA>2.0.CO;2

Vincent, E. M., Lengaigne, M., Menkes, C. E., Jourdain, N. C., Marchesiello, P., & Madec, G. (2011). Interannual variability of the South Pacific Convergence Zone and implications for tropical cyclone genesis. *Climate Dynamics*, *36*(9–10), 1881–1896. https://doi.org/10.1007/s00382-009-0716-3

Walter, R. M., Sayani, H. R., Felis, T., Cobb, K. M., Abram, N. J., Arzey, A. K., et al. (2023). The CoralHydro2k database: A global, actively curated compilation of coral $\delta^{18}O$ and Sr/Ca proxy records of tropical ocean hydrology and temperature for the common era. *Earth System Science Data*, *15*(5), 2081–2116. https://doi.org/10.5194/essd-15-2081-2023

Weber, J. N., & Woodhead, P. M. J. (1972). Temperature dependence of oxygen-18 concentration in reef coral carbonates. *Journal of Geophysical Research*, *1896–1977 77*(3), 463–473. https://doi.org/10.1029/JC077i003p00463

Weller, E., Min, S.-K., Cai, W., Zwiers, F. W., Kim, Y.-H., & Lee, D. (2016). Human-caused Indo-Pacific warm pool expansion. *Science Advances*, *2*(7), e1501719. https://doi.org/10.1126/sciadv.1501719

Wilson, R., Cook, E., D'Arrigo, R., Riedwyl, N., Evans, M. N., Tudhope, A., & Allan, R. (2010). Reconstructing ENSO: The influence of method, proxy data, climate forcing and teleconnections. *Journal of Quaternary Science*, *25*(1), 62–78. https://doi.org/10.1002/jqs.1297

Wu, H. C., Linsley, B. K., Dassié, E. P., Schiraldi, B., & deMenocal, P. B. (2013). Oceanographic variability in the South Pacific Convergence Zone region over the last 210 years from multi-site coral Sr/Ca records. *Geochemistry, Geophysics, and Geosystems*, *14*, 1435–1453. https://doi.org/10.1029/2012GC004293

Wu, Y., Fallon, S. J., Cantin, N. E., & Lough, J. M. (2021). Assessing multiproxy approaches (Sr/Ca, U/Ca, Li/Mg, and B/Mg) to reconstruct sea surface temperature from coral skeletons throughout the Great Barrier Reef. *Science Total Environment*, *786*, 147393. https://doi.org/10.1016/j.scitotenv.2021.147393

Wyrtki, K. (1989). Some thoughts about the west Pacific warm pool. In *Proceedings of the western Pacific International Meeting and Workshop on TOGA COARE* (pp. 99–109). ORSTOM.